A COMBINED ALLOSTERIC AND ATP-COMPETITIVE STRATEGY FOR ENHANCED INHIBITION OF LRRK2 IN PARKINSON'S DISEASE.

by

MINWOO LEE

(Under the Direction of Eileen J. Kennedy)

ABSTRACT

Parkinson's Disease (PD) is a progressive neurodegenerative disorder resulting in the loss of dopamine-producing neurons in the substantia nigra, leading to motor dysfunction. Current treatments manage symptoms but do not stop disease progression, emphasizing the need for novel therapies. Mutations in the LRRK2 gene are a common genetic cause of PD, with its kinase domain's hyperactivation driving neurodegeneration through impaired autophagy, mitochondrial dysfunction, and neuroinflammation. Efforts to inhibit LRRK2's kinase activity have led to the development of small-molecule inhibitors like MLi-2 (Type I) and GZD-824 (Type II). Despite their efficacy, concerns remain regarding mislocalization and toxicity. Concurrently, stapled peptides targeting LRRK2 protein-protein interactions show promise due to their enhanced stability and specificity. This study explores a combination therapy using small-molecule inhibitors and stapled peptides to suppress LRRK2 activity, aiming to identify potential synergistic effects and reduced toxicity, advancing more effective PD treatments.

INDEX WORDS: LRRK2, Parkinson's Disease, PD, Stapled peptide, MLi-2, GZD-824.

A COMBINED ALLOSTERIC AND ATP-COMPETITIVE STRATEGY FOR ENHANCED INHIBITION OF LRRK2 IN PARKINSON'S DISEASE.

By

MINWOO LEE

B.S. Kennesaw State University, USA, 2017

A Thesis Submitted to the Graduate Faculty of The University of Georgia in Partial Fulfillment of the Requirements for the Degree

MASTER OF SCIENCE

ATHENS, GEORGIA

2024

A COMBINED ALLOSTERIC AND ATP-COMPETITIVE STRATEGY FOR ENHANCED INHIBITION OF LRRK2 IN PARKINSON'S DISEASE.

By

MINWOO LEE

Major Professor: Eileen J. Kennedy

Committee: Wided Najahi Missaoui

Bin Yi

Electronic Version Approved:

Ron Walcott

Dean of the Graduate School

The University of Georgia

December 2024

DEDICATION

I dedicate this manuscript to my family, friends, and mentors. Your unwavering love, support, and encouragement have been essential in completing this journey.

To my parents, Mr. Kyuchun Lee and Mrs. Kyungnam Jeon,

Thank you for giving me the courage to rise again over the past five years after I had to relinquish everything due to my illness. Your love and support enabled me to overcome my challenges and return to pursuing my true passions.

To my sister, Sihwa Lee,

I am deeply grateful for your steadfast support, which allowed me to refocus on my studies.

To my beloved fiancé, Amuge Kim,

Your love and support have been my guiding light throughout this journey. Thank you for believing in me, for your patience, and for always encouraging me to reach for my dreams. Every achievement I celebrate reflects our shared commitment and love. I dedicate this work to you, as it represents not just my efforts, but our future together.

ACKNOWLEDGEMENTS

I would like to express my gratitude to my supervisor, Dr. Kennedy. Thank you for warmly welcoming me back to school at a late age to pursue my dreams and for allowing me to join the new research lab. Moreover, the opportunity you provided for me to work as a teaching assistant enabled me to focus more on my studies and research. Your constant encouragement, cheerful demeanor, and guidance were instrumental in helping me complete this master's program.

I also extend my thanks to my committee members, Drs. Wided Najahi Missaoui and Bin Yi, for their valuable suggestions and support. Your kindness and encouragement provided the energy I needed to navigate this journey.

Finally, I wish to thank all my lab members and the friends I have made along the way. It has been a joy to embark on this educational endeavor with you. I have learned so much from each of you and hope to return the favor one day.

LIST OF CONTENTS

page

LIST OF FIGURES / TABLES

page

CHAPTER 1

INTRODUCTION AND LITERATURE REVIEW

1.1 Parkinson's Disease (PD)

Parkinson's Disease (PD) is a progressive neurodegenerative disorder and second most prevalent neurodegenerative disease worldwide, following only by Alzheimer's. Globally, more than 10 million people are living with PD, and in the United State alone, over 90,000 new cases are diagnosed annually. This represents a 50% increase from the previously estimated 60,000 cases per year. Nearly one million people in the U.S. are living with Parkinson's Disease, and this number is expected to increase to 1.2 million by 2030. (1) The disease primarily results from the degeneration of dopamine-producing neurons in the substantia nigra, a critical brain region responsible for regulating movement. (2) Although the precise mechanisms behind this neuronal degeneration remain unknown, research has uncovered several contributing factors. Genetic mutations are implicated in 10-15% of cases, disrupting cellular processes and leading to neuron loss. Environmental exposures to toxins, herbicides, or heavy metals have also been associated with an increased risk of PD. (3) Additionally, mitochondrial dysfunction and oxidative stress contribute to neuronal damage, while neuroinflammation has been recognized as another contributing factor. (4) The development of Parkinson's Disease is believed to involve a

complex interplay of genetic predisposition, environmental influences, and age-related factors.

Currently, there are several treatment options available, including Levodopa, Dopamine Agonists, and MAO-B inhibitors. However, these treatments primarily focus on managing symptoms rather than offering a cure, aiming to replenish dopamine levels or address motor symptoms. While they provide symptomatic relief, they do not slow the progression of the disease. This highlights a significant unmet medical need, emphasizing the importance of studying pathways that may be altered throughout the disease course. Although only 10-15% of Parkinson's disease cases are linked to genetic mutations, the prevalence of PD continues to rise dramatically each year. Understanding the pathways associated with genetically linked PD could provide crucial insights for the development of innovative therapeutic targets and treatment strategies.

1.2 Leucine-Rich Repeat Kinase 2 (LRRK2)

Mutations in the Leucine-Rich Repeat Kinase 2 (LRRK2) gene are one of the most common genetic causes of Parkinson’s Disease and one of the strongest genetic risk factors in sporadic PD. (5) LRRK2 is a large 286 kDa multifunctional kinase with a complex structure consisting of several multiple domains, including Armadillo Domain (ARM), Ankyrin Repeat (ANK), Leucine-Rich Repeat (LRR), Ras Of Complex (ROC), C-terminal of ROC (COR), Kinase domain and WD40 domain. [Figure. 1] While the precise physiological roles of these domains remain unclear, (6) recent studies have identified possible

functions of them. ARM, ANK, LRR and WD40 domains are primarily involved in protein-protein interactions, whereas the LRR, ROC, COR and Kinase domains regulate LRRK2's enzymatic activity. The ROC and COR domains are related with GTPase activity, while the Kinase domain governs kinase activity. Mutations in these domains, particularly in the ROC, COR, and kinase domains, are closely associated with the development of Parkinson's disease. (7) Understanding the distinct roles of these domains provides crucial insights into how LRRK2 dysfunction contributes to neurodegeneration and explore the way for potential therapeutic strategies targeting these regions.

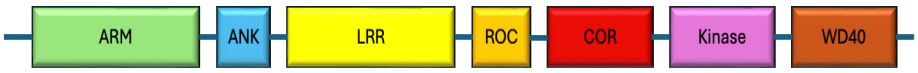

Figure 1. LRRK2 domain structure. Armadillo (ARM), Ankyrin (ANK), Leucine-rich-repeat (LRR), Ras of complex proteins (Roc), C-terminal of Roc (COR), kinase (KIN), and WD40 domains

1.3 ATP-competitive small – molecule inhibitors

Recent studies on LRRK2 have led to the introduction of ATP-competitive small-molecule inhibitors that selectively target its kinase activity. Notably, mutations in the kinase domain of the LRRK2 gene, such as G2019S, result in hyperactivation of LRRK2. This hyperactivation contributes to various pathological effects, including impaired autophagy, mitochondrial dysfunction, protein aggregation, and neuroinflammation, all of which play a significant role in the development of Parkinson's disease. (8) Kinase inhibitors are generally classified into two main categories: Type I and Type II inhibitors, based on how they interact with the kinase's active site and its conformation during binding. Type I inhibitors bind to the active conformation of the kinase (*DFG-in* state), specifically targeting the ATP-binding pocket. In contrast, Type II inhibitors bind to the inactive conformation (*DFG-out* state), not only engaging the ATP-binding pocket but also an allosteric site that is exposed only in this inactive state. (9) Type I inhibitors typically exhibit faster binding kinetics compared to Type II inhibitors. However, Type II inhibitors often provide greater selectivity due to their ability to bind the inactive conformation and adjacent allosteric sites, which helps reduce off-target effects. (10)

MLi-2 (cis-2,6-dimethyl-4-(6-(5-(1-methylcyclopropoxy)-1H-indazol-3-yl)pyrimidin-4-yl)morpholine), a well-known ATP-competitive small-molecule and Type I inhibitor, is widely regarded as the gold standard for LRRK2 inhibition. It effectively downregulates LRRK2 kinase activity, reducing oxidative stress and mitigating neuronal toxicity. (11,12) By specifically targeting the kinase domain of LRRK2, MLi-2 reduces its phosphorylation activity, which is believed to mitigate the neurodegenerative effects associated with

LRRK2 mutations, potentially slowing the progression of Parkinson's disease (PD). However, recent studies have highlighted certain limitations of MLi-2, including its tendency to induce LRRK2 mislocalization, which may disrupt vesicular trafficking, lysosomal function, and mitochondrial activity, as well as contribute to lung and kidney abnormalities. (13,14) Olverembatinib (GZD-824) is a Type II small-molecule kinase inhibitor initially studied for its effectiveness as a multi-target inhibitor, particularly against leukemia-related kinases. (15) However, its broad-spectrum activity has shown potential for inhibiting other kinases, including LRRK2. While GZD-824 is not primarily recognized for targeting LRRK2, its role as a Type II kinase inhibitor suggests potential applications in Parkinson’s disease, and ongoing research are exploring this possibility. [Figure 2]

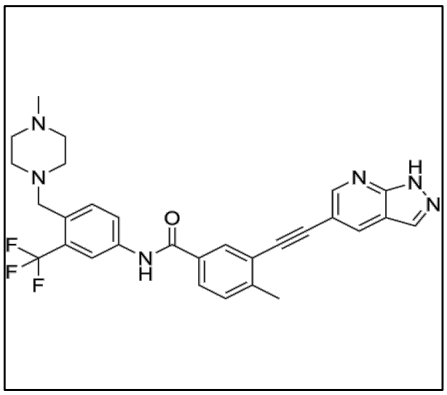

Figure 2.1. Chemical Structure of GZD-824. Chemical formula: $C_{21}H_{24}Cl_2N_4O_4S$, Molecular weight: 487.41g/mol.

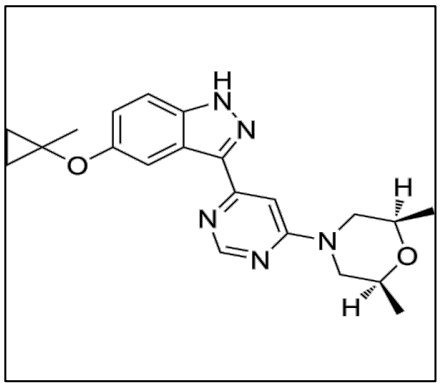

Figure 2.2. Chemical Structure of *cis*-2,6-dimethyl-4-(6-(5-(1-methylcyclopropoxy)-1*H*-indazol-3-yl)pyrimidin-4-yl)morpholine (MLi-2). Chemical formula: $C_{18}H_{19}Cl_2N_4O$, Molecular weight: 367.27g/mol.

1.4 Constrained Peptides

Over the past few years, our lab has designed and reported a library of hydrocarbon-constrained peptide mimetics targeting Protein-Protein Interactions (PPIs) of LRRK2. The hydrocarbon staple induces the linear peptide into an α-helical conformation, which typically exhibits stronger binding affinity and selectivity for its target, unlike linear peptides that make limited contacts. Additionally, stapling enhances resistance to proteolytic degradation and improves cell permeability. (16, 17) However, despite these advantages, the complexity of synthesis and optimization remains a significant challenge. Earlier studies in our lab demonstrated stapled peptides that targeting various regions of LRRK2, including the COR domain (ECOR), the ROC domain (LRIP4) and the C-terminal WD40 domain (CTIP3 and CTIP4). [Figure. 3] These stapled peptides not only downregulate kinase activity but also allosterically block the dimerization interface of LRRK2. (18, 19)

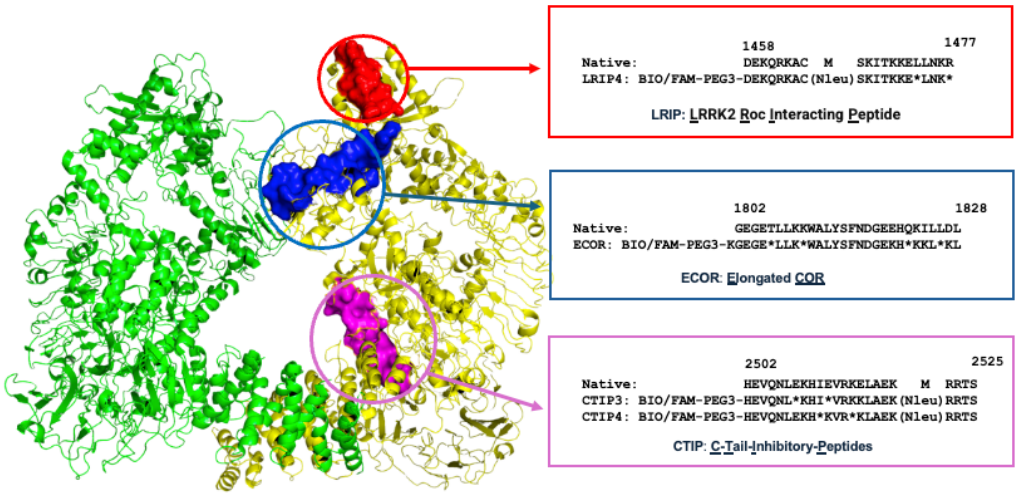

Figure 3. Full – length crystal structure of LRRK2 dimer. Highlighting the three domains where the LRIP4 (red), ECOR (blue) and CTIP3 & 4 (pink) interact with. Sequence of native and synthesized peptides used in this research. * = olefinic amino acid (S)-N-Fmoc-2-(4-pentenyl)alanine (S_5)

In this study, a combinational approach to downregulate LRRK2 kinase activity was tested using small molecule kinase inhibitors (Type I: MLi-2, Type II: GZD-824) alongside stapled peptides that have previously demonstrated the ability to downregulate LRRK2. The objective was to assess any synergistic effects when these agents were combined, while also evaluating the reduced toxicity associated with small molecule inhibitors.

CHAPTER 2

MATERIALS AND METHODS.

2.1 Peptide Synthesis

The list of reagents used in peptides synthesis is provided in Table 1.

The peptide was synthesized using the Fmoc Solid-Phase Peptide Synthesis (SPPS) method, sequentially coupling N-α-Fmoc-protected amino acids onto a rink amide MBHA resin. Before the addition of the first amino acid residue, approximately 1 mL of N-methyl-pyrrolidinone (NMP) was added to the resin and bubbled for 10 minutes to allow the resin to swell and equilibrate, optimizing conditions for coupling. Afterward, the NMP was drained, and 1 mL of deprotection solution (containing 25% piperidine and 75% NMP) was added to the resin and bubbled for 25 minutes to remove the Fmoc group. Following this deprotection step, the solution was drained, and the resin, along with the sides of the column, was washed with NMP for 30 seconds, with bubbling repeated three times.

For the amino acid coupling, 0.5 mL of amino acid solution (10 equivalents) was added first, followed by 0.495 mL of HCTU solution (9.9 equivalents), in that specific order, to avoid premature capping of the peptide. It's crucial to ensure that the amino acid solution is added before the HCTU, as adding HCTU first would cap the peptide and prevent further

residues from being added. Afterward, 87 µL of DIEA (20 equivalents) was introduced into the mixture, and the solution was bubbled for 45 minutes.

After 45 minutes, the column was drained and washed with 1 mL of NMP, thoroughly rinsing the sides of the column for 30 seconds bubbling per wash, repeated three times. For the coupling of the olefinic amino acid (S)-N-Fmoc-2-(4-pentenyl)alanine (S_5), 200 µL of olefinic amino acid (4 equivalents) was added, followed by 198 µL of HCTU and 43.5 µL of DIEA (10 equivalents), in that order.

To connect the S_5 amino acids on the sequence, ring-closing-metathesis (RCM) was performed. The resin was washed by 1,2-dichloroethane (DCE) by bubbling for 30 seconds, repeated three times. After the washes, the resin was allowed to equilibrate by bubbling for 10 minutes. Following equilibration, the DCE was drained, and 1mL (0.4 equivalents) of cyclization solution containing Grubbs 1st catalyst dissolved in DCE was added and bubbled for one hour. This reaction was repeated twice to ensure complete cyclization. After the two reactions, column was drained and washed with DCM for 30 seconds, repeated three times, followed by wash with NMP three times for 30 seconds. Finally, the resin was equilibrated in NMP.

Peptides were labeled with either fluorescein or biotin for quantification and for certain experiments. Following the final deprotection and washes, 1mL of DMF was added and allowed to equilibrate by bubbling for at least 10 minutes. For the fluorescein labeling, 1mL of fluorescein solution composed of 19mg of fluorescein (2 equivalents) and 19mg of HCTU (1.8 equivalents) dissolved in DMF, was added to the resin, and begin bubbling.

Subsequently, 20µL of DIEA (4.6 equivalents) was added. This reaction was conducted under foil cover to keep protect it from light. After 1 to 2 hours of bubbling, an additional 20µL of DIEA was added, and the mixture was allowed to bubble overnight, remaining covered with foil. For the biotin labeling, 61mg of biotin (10 equivalents) and 109mg of HCTU (9.9 equivalents) were dissolved in a 1.2mL solution composing a 1:1 ratio of DMSO and DMF. Following the addition of the biotin/HCTU solution, 75µL of DIEA was added after 1 to 2 hours of bubbling and the reaction allowed to continue bubbling overnight. The following day, the resin was sequentially washed three times with DMF, DCM, diethyl ether, and methanol. After the final methanol wash, both the column and resin were rinsed with diethyl ether and left to air-dry. Once fully dried, the resin was transferred to a reaction vial, and 1.5 mL of cleavage solution (95% TFA, 2.5% TIS, and 2.5% water) was added. The vial was placed on a rotisserie and rotated for 4 hours. After this period, the peptide was filtered into 3 mL of t-butyl methyl ether (TBME) using a syringe packed with a small ball of glass wool. The filtrate was then centrifuged at 2800 rpm for 30 minutes at 4°C to separate the peptide pellet from the supernatant. [Figure 4] (20).

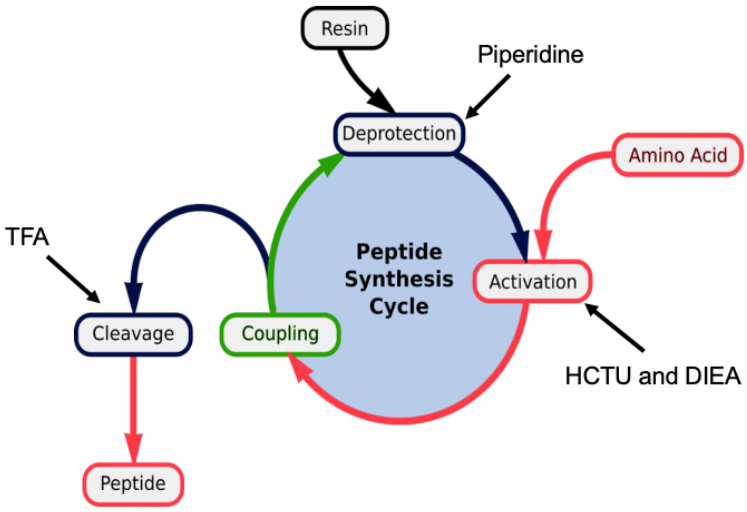

Figure 4. Fmoc Solid Phase Peptide Synthesis cycle. The free N-terminal amine of a solid-phase attached peptide is coupled to a single N-protected amino acid unit. This unit is then deprotected, revealing a new N-terminal amine to which a further amino acid may be attached.

Reagent Name	Vendor
Rink Amide MBHA Resin	Novabiochem
N-α-Fmoc acid amino acids	Novabiochem
(S)-N-Fmoc-2-(4-pentenyl)alanine (S_5)	Sigma - Aldrich
N-methyl-pyrrolidinone (NMP)	Fisher Scientific
O-(1*H*-6-Chlorobenzotriazole-1-yl)-1,1,3,3-tetramethyluronium hexafluorophosphate (HCTU)	Oakwood Chemical
Dissopropylethylamine (DIEA)	Fisher Scientific
1,2-dichloroethane (DCE)	Fisher Scientific
dichloromethane (DCM)	Fisher Scientific
Grubb's 1st catalyst	Sigma - Aldrich
dimethyl sulfoxide (DMSO)	Fisher Scientific
dimethylformamide (DMF)	Fisher Scientific
trifluoroacetic acid (TFA)	Fisher Scientific
triisopropylsilane (TIS)	Fisher Scientific
methyl-tert-butyl ether (MTBE)	Fisher Scientific
diethyl ether	Fisher Scientific
Methanol	Honeywell

Table 1. list of reagents used in peptides synthesis and its vendor.

2.2 Peptide Identification

The peptide pellet was dissolved in 1 mL of methanol and filtered into a glass HPLC vial using a 0.45 µm filter. The peptide was analyzed using Electrospray Ionization Mass Spectrometry (ESI-MS) (Agilent, 6120 Single Quadrupole). For the MS analysis, mobile phases consisted of 0.1% TFA in water and 0.1% TFA in acetonitrile, with an injection volume of 30 µL and a flow rate of 0.5 mL/min. After confirming the correct peptide mass, the retention time was recorded for the subsequent purification process. Reversed-Phase High-Performance Liquid Chromatography (RP-HPLC) (Thermo scientific, Dionex Ultimate 3000) with an SB-C18 semi-prep column (Zorbax) was employed for peptide purification. Mobile phases A and B were 0.1% TFA in water and 0.1% TFA in acetonitrile, respectively. A 10-100% gradient was used at a flow rate of 4 mL/min.

2.3 Peptide Quantification

Synthesized and purified peptides were analyzed using a Synergy 2 plate reader. For the biotin-labeled peptides, a 2-hydroxyazobenzene-4'-carboxylic acid (HABA)-avidin complex (Thermo Fisher) was employed, with absorbance measured at 500 nm. Quantification was based on the decrease in absorbance of the HABA-avidin complex in the absence and presence of the peptide. For the FAM-labeled peptides, a 10 mM Tris buffer (pH 8.0) served as the medium, with methanol as the blank, and absorbance was measured at 495 nm for quantification.

2.4 Cell Culture

A549 human lung adenocarcinoma cells (ATCC, CCL185) were cultured in Roswell Park Memorial Institute (RPMI; Lonza) medium, supplemented with 10% of Fetal Bovine Serum (FBS; Sigma-Aldrich) and 1% penicillin (Gibco). Cells were maintained in a 37°C incubator with 5% CO_2.

For subculturing, cells were washed with phosphate-buffered saline (PBS) to remove residual media. After aspiration of PBS, 3mL of Trypsin-EDTA (Gibco) was added to the cell culture plate, and cells were incubated at 37°C for 3 – 5 minutes to facilitate detachment. Complete detachment was confirmed by gently tapping the plate and observing the cells under a microscope. Trypsin was neutralized by adding 6mL of fresh medium, and the cell suspension was transferred to a 15mL conical tube. Cells were then pelleted by centrifugation at 1,200 rpm for 5 minutes. After centrifugation, the supernatant was discarded, and the pellet was resuspended in fresh growth medium, and cells were counted using hemocytometer. Cells were seed at a density of 1.5×10^6 cells per 10cm cell culture plate. The medium was replaced every 2 – 3 days, and cells were passaged upon reaching 80 – 90% confluency.

2.5 Rab Immunoblotting

Approximately 0.5×10^6 A549 cells were seeded per well in a 6-well plate and cultured in complete RPMI growth medium until reaching 80% confluency. Once the cells were ready, they were treated with 2.5μM of each peptide (LRIP4, ECOR, CTIP3 and CTIP4) for 6 hours. For combination treatment, 0.5μM of MLi-2 was added 2 hours before cell harvesting, in addition to the respective peptide treatments. Untreated A549 cells served as a positive control, while 0.5μM MLi-2 was used as a negative control. After treatment, cells were

lysed with 1X Laemmli buffer and harvested on ice. Lysates were heated at 90–95°C for 10 minutes in a heat block, followed by centrifugation for 30 seconds. The samples were then stored at -20°C for subsequent experiments. The same procedures were followed for the GZD-824 experiment, except GZD-824 was added simultaneously with the peptides for 6 hours.

For electrophoresis, a 15-well polyacrylamide gel was prepared with a 12% separating layer and a 6% stacking layer. A total of 5 µL of PageRuler Prestained Protein Ladder (Thermo Scientific, 26616) was used as the molecular weight marker, and 15 µL of each sample were loaded. The gel was run in 1X Towbin's running buffer at 120 V. To minimize heat-induced band distortion or tilting, the electrophoresis tank was placed on ice during the run.

Protein transfer was carried out using the semi-dry transfer method with the Trans-Blot Turbo system (BIO-RAD). Bjerrum Schafer-Nielsen Buffer (48 mM Tris, 39 mM glycine, 20% methanol, pH 9.2) was used for the transfer. The transfer was performed at 0.2 A and 25 V for 45 minutes.

Following the protein transfer, the membrane was cut just above the 25 kDa marker to separate the regions containing the α-tubulin and Rab proteins, minimizing nonspecific binding. The two membrane sections were blocked with 3% bovine serum albumin (BSA; Sigma-Aldrich) for 1–2 hours at room temperature. After blocking, the α-tubulin membrane was incubated with a 1:2000 dilution of α-tubulin primary antibody (DM1A Mouse mAb #3873, Cell Signaling Technology), while the Rab membrane was incubated with a 1:1000 dilution of pRab10 (phospho T73, Abcam ab230261, MJF-R21) primary antibody. Both membranes were incubated overnight at 4°C with gentle rocking. The following day, the membranes were washed by rocking at room temperature in 1X TBST for a total of five washes, each lasting 5 minutes. After washing, the secondary antibodies were applied for 2 hours: a 1:15,000 dilution of Goat Anti-Rabbit secondary antibody (LiCOR,

800CW) for the Rab antibodies and a 1:15,000 dilution of Donkey Anti-Mouse secondary antibody (LiCOR, 680RD) for the α-tubulin. After 2 hours of 2nd antibody treatment, the membranes were washed with 1X TBST three times, 10 minutes each. All blots were then imaged using a Li-COR imager at wavelengths of 600, 700, and 800 nm. After imaging the pRab10 blots, the Rab membrane was reprobed with a 1:1000 dilution of tRab10 primary antibody (Abcam, ab237703, MJF-R23) overnight and imaged the next day following the same procedures.

The resulting images were quantified using Image Studio software and normalized to Positive and negative controls. Statistical analysis was performed using One-Way ANOVA on GraphPad Prism, comparing each treatment to the untreated control. Significance levels were defined as follows: n.s.=not significant, * = $p< 0.05$, ** = $p< 0.01$, *** = $p< 0.001$, and **** = $p< 0.0001$.

CHAPTER 3

RESULTS AND DISCUSSION

The peptides used in this study were designed based on a detailed analysis of the full-length LRRK2 structure and its dynamic transition between monomeric and dimeric states. [Figure. 2] Potential key regions involved in protein-protein interactions (PPIs), critical for LRRK2 dimerization, were identified and targeted. From this effort, four critical peptides were highlighted from distinct domains of LRRK2: LRIP4 for the ROC domain, ECOR for the COR domain, and CTIP3 and CTIP4 for the C-tail of the WD40 domain. These peptides are mimicking the sequences of their specific domains and modified to have better characteristics in term of stability, cell permeability and solubility. The incorporation of olefinic amino acid (pentenyl alanine, S_5) residues in these peptides promoted a helical secondary structure through constrained hydrocarbon chains. This stapling process overcome the limits of linear formation of peptide, including, susceptibility to proteolysis, limited binding affinity to target protein. Additionally, the triethylene glycol (PEG3) linker molecule at the N-terminal of these stapled peptides enhanced their hydrophobicity and solubility without significantly altering the overall molecular size. This modification allows the peptides to balance hydrophobic and hydrophilic properties, improving their circulation and effectiveness within biological systems. (21)

After synthesizing the four peptides, their chemical structures were drawn using ChemDraw, and their expected molecular weights were calculated and confirmed through Electrospray Ionization Mass Spectrometry (ESI-MS). [Table. 2] Following the initial mass spectrometry analysis, the peptides were purified using reverse-phase high-performance liquid chromatography (RP-HPLC) to

eliminate any peptide debris or byproducts that could lead to nonspecific binding in subsequent experiments. After purification, a final mass spectrometry analysis was conducted, and peptide quantification was performed to determine the exact concentrations of the peptides. [Figure. 5]

Peptides Name	Sequence	Expected Molecular Weight (g/mol)	
		FAM - labeled	BIO - labeled
LRIP4	(BIO/FAM)-PEG3-DEKQRKAC(Nleu)SKITKKE*LNK*	2929.4	2797.4
ECOR	(BIO/FAM)-PEG3-KGEGE*LLK*WALYSFNDGEKH*KKL*KL	3979.6	3847.6
CTIP3	(BIO/FAM)-PEG3-HEVQNL*KHI*VRKKLAEKXRRTS	3479.9	3347.9
CTIP4	(BIO/FAM)-PEG3-HEVQNLEKH*KVR*KLAEKXRRTS	3495.9	3363.9

Table 2. Sequences and expected molecular weights of peptides used in this research.

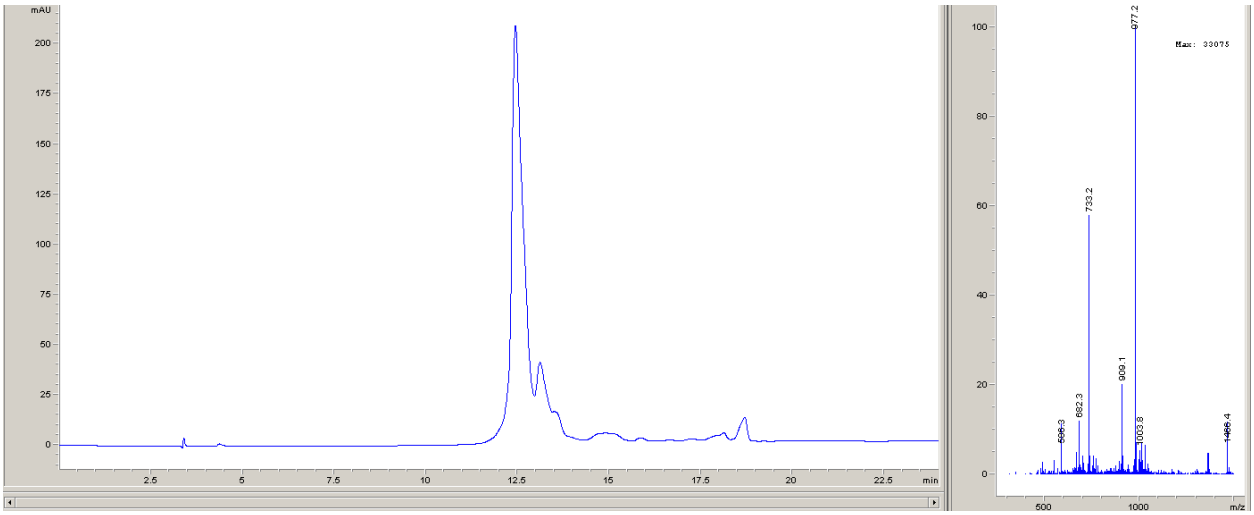

Figure 5.1. ESI-Mass Spectrometry Analysis of FAM-labeled LRIP4 FAM-PEG3-DEKQRKAC(Nleu)SKITKKE*LNK*, actual weight: 2928.8 (expected weight: 2929.4)

* represents (S)-N-Fmoc-2-(4-pentenyl) alanine.

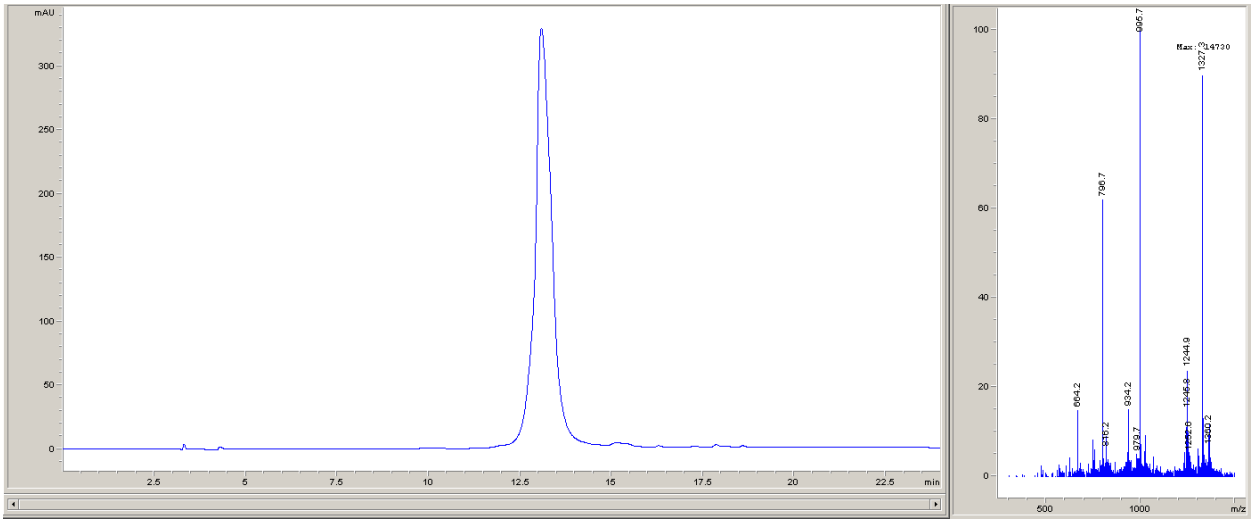

Figure 5.2. ESI-Mass Spectrometry Analysis of FAM-labeled ECOR, FAM-PEG3-KGEGE*LLK*WALYSFNDGEKH*KKL*KL, actual weight: 3986.8 (expected weight: 3979.6)

* represents (S)-N-Fmoc-2-(4-pentenyl) alanine.

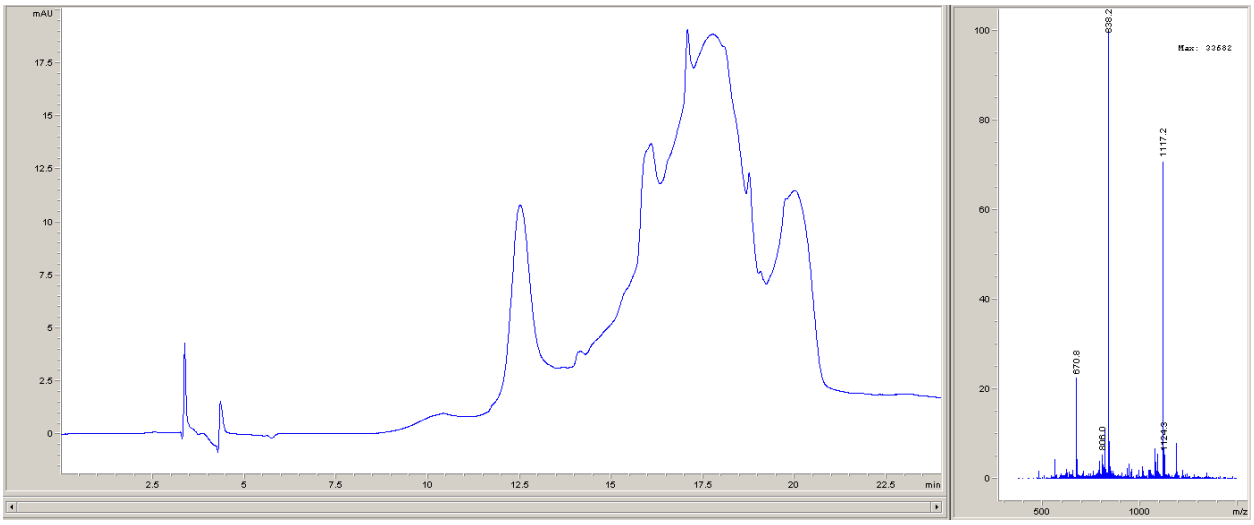

Figure 5.3. ESI-Mass Spectrometry Analysis of Bio-labeled CTIP3, BIO-PEG3-HEVQNL*KHI*VRKKLAEKXRRTS, actual weight: 3348.8 (expected weight: 3347.9)

* represents (S)-N-Fmoc-2-(4-pentenyl) alanine.

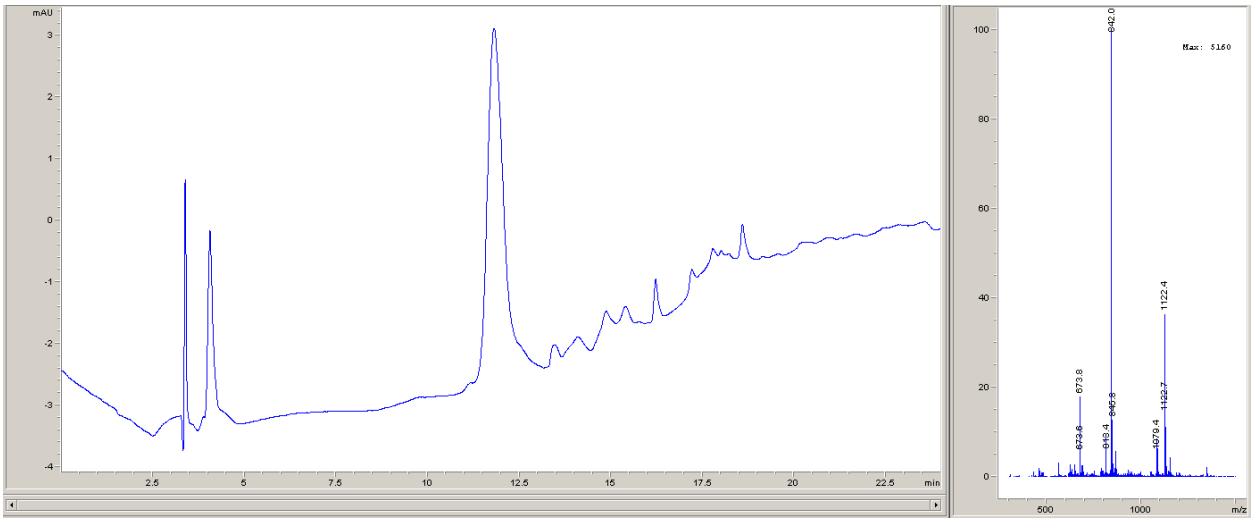

Figure 5.4 ESI-Mass Spectrometry Analysis of Bio-labeled CTIP4, BIO-PEG3-HEVQNLEKH*KVR*KLAEKXRRTS, actual weight: 3364.0 (expected weight: 3363.9)

* represents (S)-N-Fmoc-2-(4-pentenyl) alanine.

Following the confirmation of successful peptide synthesis, we evaluated the ability of the peptides, in combination with ATP-competitive small molecule kinase inhibitors (Type I and Type II), to affect LRRK2 kinase activity, which is associated with Parkinson's disease. Each peptide (2.5 μM) and a combination of each peptide (2.5 μM) with either 0.5 μM of Type I or Type II inhibitor were incubated in A549 cells at 37°C for 6 hours. The cells were then lysed and prepared for western blotting. Previous studies have shown that these peptides downregulate LRRK2 kinase activity when they react on solely. (18,19) [Figure 6]

In this study, we explored the potential synergistic effects between peptides, which have previously demonstrated downregulation activity, and ATP-competitive small molecule inhibitors (MLi-2 or GZD-824) using a combinational approach. After triplicate runs, signals were quantified using Image Studio, and the mean intensity values were calculated as described below. These values were then normalized against the untreated control. The normalized data were subsequently analyzed using one-way ANOVA tool in PRISM software.

$$mean\ intensity = \frac{(pRab10\ T73\ signal/Alpha - tubulin\ signal)}{(Total\ Rab10\ signal/\ Alpha - tubulin\ signal)}$$

Of the four peptides tested, three exhibited approximately 50–70% downregulation of LRRK2 autophosphorylation at a concentration of 2.5 μM. LRIP4, however, did not show a statistically significant decrease in activity at this concentration. This result is consistent with previous findings, where LRIP4 demonstrated a 50% downregulation at a higher concentration of 10 μM. [Figure 7]

In evaluating the combination approach, all peptide and small-molecule inhibitor combinations demonstrated approximately 80% downregulation of LRRK2 kinase activity. However, it was unclear

whether this effect was due to the synergy between the peptides and the inhibitor, or primarily driven by the small-molecule inhibitor alone. To clarify this, additional statistical analysis was conducted by normalizing the data to the small-molecule inhibitor and comparing its effects alone versus in combination with peptides.

This analysis revealed that pairing CTIP3 or CTIP4 with MLi-2 significantly improved the downregulation of LRRK2 kinase autophosphorylation. In contrast, combinations involving LRIP4 or ECOR with MLi-2 did not show statistically significant improvements. Additionally, none of the peptide combinations with GZD-824 produced meaningful data, suggesting a lack of synergistic effects with this particular inhibitor. [Figure. 8]

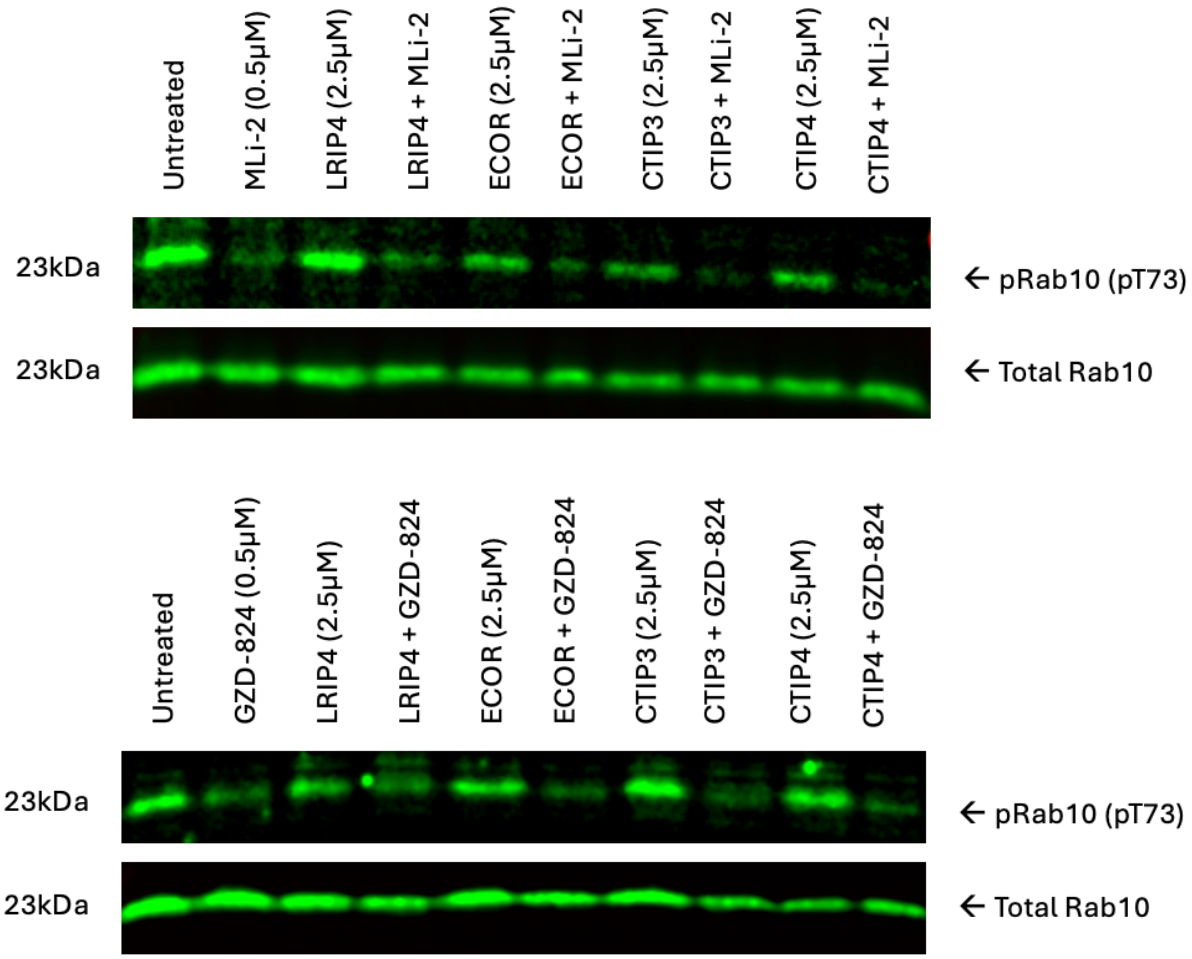

Figure 6. Rab10 phosphorylation with 4 peptides and combination of MLi-2 or GZD-824 treatments. 6hr. A549 cells with Rab10 were used to investigate the inhibitory effects of LRIP4, ECOR, CTIP3 and CTIP4 (2.5μM) and combination with MLi-2 (0.5μM) or GZD-824 (0.5μM) on endogenous LRRK2 kinase activity as measured by Rab10 phosphorlyation. (n=3)

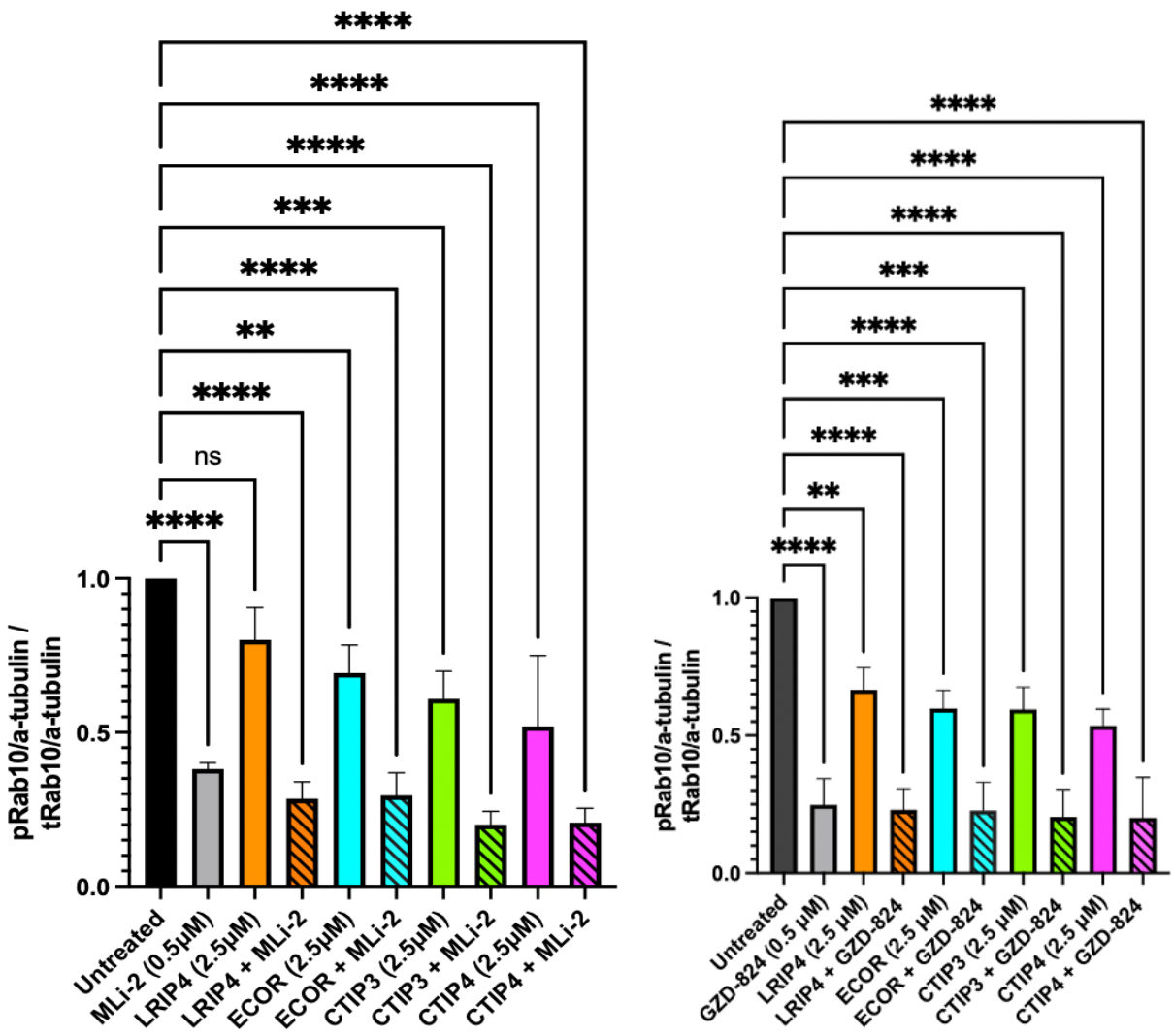

Figure 7. quantification of western blot; normalized to untreated.

Peptides treated individually resulted in approximately 50–70% downregulation of LRRK2 autophosphorylation at 2.5 μM. However, LRIP4 showed less downregulation activity compared to the other tested peptides at this concentration.

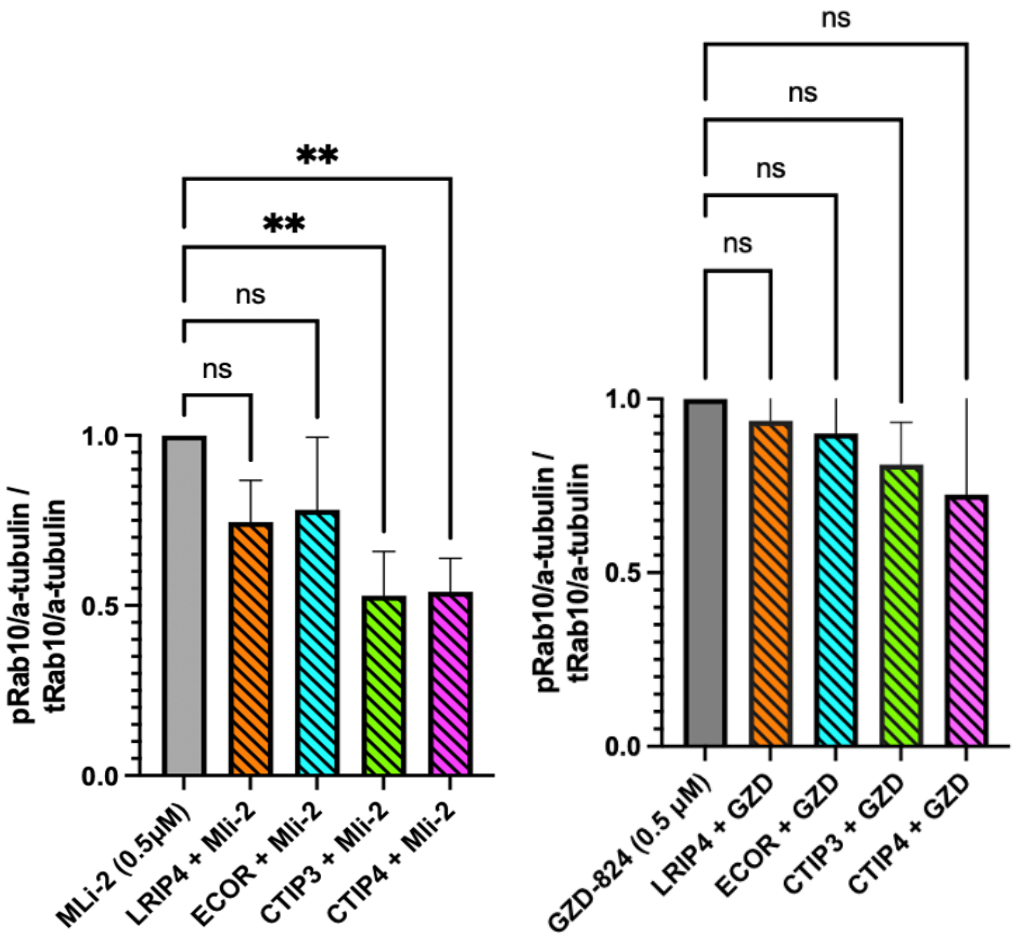

Figure 8. quantification of western blot; normalized to controls.

Combining MLi-2 with CTIP3 and CTIP4 resulted in a 50% greater downregulation of activity compared to MLi-2 alone. While other combinations also demonstrated downregulation, these effects were not statistically significant. For GZD-824 combinations, none of the pairings showed a statistically significant improvement in downregulation.

CHAPTER 4

CONCLUSION AND FUTURE STUDY

With the full-length structure of LRRK2 revealed, specific regions within its distinct domains involved in dimerization—frequently observed in Parkinson's disease (PD) patients—were identified and studied for their role in LRRK2's abnormal function, a key contributor to disease pathology. (22) In recent years, extensive research has focused on constrained peptides designed to mimic the sequences of these critical regions. These peptides have been utilized to interfere with the dimerization process, ultimately aiming to disrupt and downregulate LRRK2 kinase activity.

In parallel, ATP-competitive small-molecule inhibitors, such as MLi-2 and GZD-824, have become standard approaches for inhibiting LRRK2 kinase activity in Parkinson's disease research. (23) While these inhibitors are effective, they present challenges, particularly regarding side effects. Currently, many new small-molecule inhibitors are being developed alongside peptides designed to mimic sequences from other LRRK2 domains that may be involved in PD progression and pathology. (24)

In this study, we explored a combinational approach by pairing peptides—previously shown to downregulate LRRK2 kinase activity—with the established inhibitor MLi-2. Despite MLi-2's efficacy, its side effects remain a concern. Our findings demonstrated that combining these treatments can produce a synergistic effect, with statistically significant

improvements in downregulation observed when CTIP3 or CTIP4 was paired with MLi-2. These results open new possibilities for future research into diverse treatment strategies and provide valuable insights into developing novel therapeutic approaches for addressing Parkinson's disease by selectively modulating LRRK2 activity through combination treatments.

For future investigations, it will be important to determine the optimal concentration of CTIP3 or CTIP4 in combination with MLi-2 that still yields significant improvements in LRRK2 downregulation. Once this optimal concentration is identified, subsequent studies should focus on evaluating the reduction of side effects typically associated with the traditional use of MLi-2. Additionally, exploring whether combining peptides from different LRRK2 domains could lead to enhanced synergy—or whether their downregulating activities may counteract each other—would be an intriguing avenue for further research.

At this point, an effective cure for Parkinson's disease has yet to be developed, I hope that research like this, which explores new approaches, will pave the way to overcome Parkinson's disease and bring hope to those affected.

REFERENCE

1. Marras, C., Beck, J.C., Bower, J.H. *et al.* Prevalence of Parkinson's disease across North America. *npj Parkinson's Disease* **4**, 21 (2018). https://doi.org/10.1038/s41531-018-0058-0

2. Liu, L., Cui, Y., Chang, YZ. *et al.* Ferroptosis-related factors in the substantia nigra are associated with Parkinson's disease. *Sci Rep* **13**, 15365 (2023).

3. Pyatha S, Kim H, Lee D, Kim K. Association between Heavy Metal Exposure and Parkinson's Disease: A Review of the Mechanisms Related to Oxidative Stress. *Antioxidants (Basel)*. 2022;11(12):2467. Published 2022 Dec 15. doi:10.3390/antiox11122467

4. Moon HE, Paek SH. Mitochondrial Dysfunction in Parkinson's Disease. *Exp Neurobiol*. 2015;24(2):103-116. doi:10.5607/en.2015.24.2.103

5. Xiong Y, Dawson TM, Dawson VL. Models of LRRK2-Associated Parkinson's Disease. *Adv Neurobiol*. 2017;14:163-191. doi:10.1007/978-3-319-49969-7_9

6. Li, JQ., Tan, L. & Yu, JT. The role of the LRRK2 gene in Parkinsonism. *Mol Neurodegeneration* **9**, 47 (2014). https://doi.org/10.1186/1750-1326-9-47

7. Zhang X, Kortholt A. LRRK2 Structure-Based Activation Mechanism and Pathogenesis. *Biomolecules*. 2023;13(4):612. Published 2023 Mar 28. doi:10.3390/biom13040612

8. Kelly K, Wang S, Boddu R, Liu Z, Moukha-Chafiq O, Augelli-Szafran C, West AB. The G2019S mutation in LRRK2 imparts resiliency to kinase inhibition. Exp Neurol. 2018 Nov;309:1-13. doi: 10.1016/j.expneurol.2018.07.012. Epub 2018 Jul 24. PMID: 30048714; PMCID: PMC7041630.

9. Zhao, Z., Bourne, P.E. (2020). Overview of Current Type I/II Kinase Inhibitors. In: Shapiro, P. (eds) Next Generation Kinase Inhibitors. Springer, Cham. https://doi.org/10.1007/978-3-030-48283-1_2

10. Deng, X., Choi, H. G., Buhrlage, S. J., & Gray, N. S. (2012). Leucine-rich repeat kinase 2 inhibitors: a patent review (2006 – 2011). *Expert Opinion on Therapeutic Patents*, *22*(12), 1415–1426.

11. Bhujbal SP, Jun J, Park H, Moon J, Min K, Hah J-M. Gaining Insights into Key Structural Hotspots within the Allosteric Binding Pockets of Protein

Kinases. *International Journal of Molecular Sciences*. 2024; 25(9):4725. https://doi.org/10.3390/ijms25094725

12. Sanz Murillo M, Villagran Suarez A, Dederer V, et al. Inhibition of Parkinson's disease-related LRRK2 by type I and type II kinase inhibitors: Activity and structures. *Sci Adv*. 2023;9(48):eadk6191. doi:10.1126/sciadv.adk6191

13. Roberto Di Maio *et al.* LRRK2 activation in idiopathic Parkinson's disease. *Sci. Transl. Med.***10**, eaar5429(2018). DOI:10.1126/scitranslmed.aar5429

14. Reina N. Fuji *et al.,* Effect of selective LRRK2 kinase inhibition on nonhuman primate lung. *Sci. Transl. Med.***7**,273ra15 273ra15 (2015). DOI:10.1126/scitranslmed.aaa3634

15. Ye W, Jiang Z, Lu X, et al. GZD824 suppresses the growth of human B cell precursor acute lymphoblastic leukemia cells by inhibiting the SRC kinase and PI3K/AKT pathways. *Oncotarget*. 2016;8(50):87002-87015. Published 2016 Jul 28. doi:10.18632/oncotarget.10881

16. Li X, Chen S, Zhang WD, Hu HG. Stapled Helical Peptides Bearing Different Anchoring Residues. Chem Rev. 2020 Sep 23;120(18):10079-10144. doi: 10.1021/acs.chemrev.0c00532. Epub 2020 Aug 14. PMID: 32794722.

17. Li X, Zou Y, Hu H. Different stapling-based peptide drug design: Mimicking *α*-helix as inhibitors of protein–protein interaction. *Chinese Chemical Letters*. 2018 July; 29(7):1088-1092. DOI: 10.1016/j.cclet.2018.01.018

18. Pathak P, Alexander KK, Helton LG, Kennedy EJ, et al. Doubly Constrained C-terminal of Roc (COR) Domain-Derived Peptides Inhibit Leucine-Rich Repeat Kinase 2 (LRRK2) Dimerization. ACS Chem Neurosci. 2023 Jun 7;14(11):1971-1980. doi: 10.1021/acschemneuro.3c00259. Epub 2023 May 18. PMID: 37200505; PMCID: PMC10251477.

19. Helton LG, Soliman A, Kennedy EJ, et al. Allosteric Inhibition of Parkinson's-Linked LRRK2 by Constrained Peptides. ACS Chem Biol. 2021 Nov 19;16(11):2326-2338. doi: 10.1021/acschembio.1c00487. Epub 2021 Sep 8. PMID: 34496561.

20. Antibodies-online. (n.d.). [Solid-Phase Peptide Synthesis SPPS]. antibodies-online. Retrieved from https://www.antibodies-online.com/resources/17/5034/peptide-synthesis-methods-and-reagents/

21. Hoang Thi, T.T.; Pilkington, E.H.; Nguyen, D.H.; Lee, J.S.; Park, K.D.; Truong, N.P. The Importance of Poly(ethylene glycol) Alternatives for Overcoming PEG Immunogenicity in Drug Delivery and Bioconjugation. *Polymers* **2020**, *12*, 298. https://doi.org/10.3390/polym12020298

22. Li X, Ye M, Wang Y, Qiu M, Fu T, Zhang J, Zhou B, Lu S. How Parkinson's disease-related mutations disrupt the dimerization of WD40 domain in LRRK2: a comparative molecular dynamics simulation study. Phys Chem Chem Phys. 2020 Sep 23;22(36):20421-20433. doi: 10.1039/d0cp03171b.

23. Snead, D.M., Matyszewski, M., Dickey, A.M. *et al.* Structural basis for Parkinson's disease-linked LRRK2's binding to microtubules. *Nat Struct Mol Biol* **29**, 1196–1207 (2022). https://doi.org/10.1038/s41594-022-00863-y

24. Taymans, JM., Fell, M., Greenamyre, T. *et al.* Perspective on the current state of the LRRK2 field. *npj Parkinsons Dis.* **9**, 104 (2023). https://doi.org/10.1038/s41531-023-00544-7